Discover Materials

Research

One-vs-One, One-vs-Rest, and a novel Outcome-Driven One-vs-One binary classifiers enabled by optoelectronic memristors towards overcoming hardware limitations in multiclass classification

George Psaltakis[1] · **Konstantinos Rogdakis**[1,2] · **Michalis Loizos**[1] · **Emmanuel Kymakis**[1,2]

Received: 6 September 2023 / Accepted: 26 February 2024
Published online: 03 March 2024

Abstract
Deep neural networks have achieved considerable success over the past ten years in a variety of fields. However, current state-of-the-art artificial intelligence (AI) systems require large computing hardware infrastructure and high power consumption. To overcome these hurdles, it is required to adopt new strategies such as designing novel computation architectures and developing building blocks that can mimic the low energy consumption of biological systems. On the architecture level, implementing classification tasks by splitting the problem into simpler subtasks is a way to relax hardware constraints despite the less accuracy of the approach. On the computation unit level, memristive devices are a promising technology for low power neuromorphic computation. Hereby, we combine both these two approaches and present a novel algorithmic approach for multiclass classification tasks through splitting the problem into binary subtasks while using optoelectronics memristors as synapses. Our approach leverages the core fundamentals from the One-vs-One (OvO) and the One-vs-Rest (OvR) classification strategies towards a novel Outcome-Driven One-vs-One (ODOvO) approach. The light modulation of synaptic weights, fed in our algorithm from experimental data, is a key enabling parameter that permits classification without modifying further applied electrical biases. Our approach requires at least a 10X less synapses (only 196 synapses are required) while reduces the classification time by up to $\frac{N}{2}$ compared to conventional memristors. We show that the novel ODOvO algorithm has similar accuracies to OvO (reaching over 60% on the MNIST dataset) while requiring even fewer iterations compared to the OvR. Consequently, our approach constitutes a feasible solution for neural networks where key priorities are the minimum energy consumption i.e., small iterations number, fast execution, and the low hardware requirements allowing experimental verification.

1 Introduction

Pattern recognition through multiclass classification constitutes a very important field in recent years that has led to many technological and societal advancements thanks to its progression. Numerous technological applications have been developed focusing on human healthcare and well-being [1] to optical character detection [2], to voice

Supplementary Information The online version contains supplementary material available at https://doi.org/10.1007/s43939-024-00077-7.

✉ Konstantinos Rogdakis, krogdakis@hmu.gr; ✉ Emmanuel Kymakis, kymakis@hmu.gr; George Psaltakis, th20027@edu.hmu.gr; Michalis Loizos, mloizos@hmu.gr | [1]Department of Electrical & Computer Engineering, Hellenic Mediterranean University (HMU), 71410 Heraklion, Crete, Greece. [2]Institute of Emerging Technologies (I-EMERGE), University Research and Innovation Center, HMU, 71410 Heraklion, Crete, Greece.

recognition to even face and fingerprint recognition [3, 4]. Current state-of-the-art artificial intelligence (AI) systems such as DeepMind's AlphaGo consume up to ~ 10 MW compared to only 20W of human brain operation [5]. Despite the incredible progression of AI over the years across various applications, it is required to adopt new strategies in designing materials, devices, architectures, and algorithms to mimic low energy consumption per operation of biological systems while reducing the manufacturing cost [6–11]. To overcome these hurdles, on the architecture level, implementing classification tasks by splitting the problem into simpler subtasks is a way to relax hardware constraints despite the less accuracy of the approach. On the computation unit level, memristive devices are an ideal platform to implement on hardware-level deep neural networks compatible with low power consumption. Neural networks have demonstrated significant potential for implementing low-energy pattern recognition in neuromorphic hardware, such as memristor crossbars. However, conventional algorithmic approaches require neural networks consisting of thousands of synapses and neurons, making them very hardware and energy intensive, prohibiting any experimental verification of the models. Recent advancements have been based on different techniques for pattern recognition applications such as implementing various algorithms for problems classification on memristors and analogue electronics that have tunable weights [12]. The challenge still lies in the demanding hardware requirements necessary to support these hardware accelerators for pattern recognition and other AI applications. Reducing the number of memristors is thus a critical need for practical applications with minimal energy consumption. Algorithmic strategies, like the one-vs-one (OvO) and one-vs-rest (OvR) binary to multiclass classification can assist in partitioning the classification into multiple smaller problems. New algorithmic approaches and hardware configurations however should be developed to address this energy deluge and complexity.

Neuromorphic computing is an ever-evolving field that aims to mimic the neural structure and function of the brain, with high energy efficiency by adopting an in-memory-processing scheme [13, 14] that could enable systems to perform local learning and decision-making paving the way for applications in Internet of Things (IoT) sensors and autonomous robots. [5, 6, 15–18] This strategy will reduce the energy consumption and the dependency on the time-consuming cloud communication. Specifically, the gradual resistance changes in memristors induced by electrical voltage pulses resemble the continuous synaptic weight changes in biological systems, hence a variety of synaptic functionalities can be emulated [19]. Memristors can be used as synapses (requiring non-volatile operation mode) or even emulating neuron activity (volatile operation mode) in any neuromorphic computing system. Notably, optoelectronic memory devices for neuromorphic computing provide concrete advantages such as low energy consumption and smaller delays, high-speed non-destructive read method not dependent on electrical wires that solves crosstalk issues [19], visual sensing, and signal processing[7, 20, 21], and logic operations[22]. Optoelectronic memristors can act as the artificial retina and combine optical sensing and high-level image processing toward artificial visual systems [23], as well as can be used to develop optical neurons, aside to synaptic function, extending further their application domains. By incorporating both light and electric modularity, optoelectronic memristors could resemble the multi-modal sensory nature of biological systems[24], as they can directly sense optical signals[25] and use them to control their resistance state [23, 26]. The light modulation of the synaptic weight of optoelectronic memristors could permit the implementation of computation tasks without requiring changing further the applied electrical bias on various memristive nodes, offering therefore the potential for lowering the number of required memristors in the chip. Various materials have been implemented for optoelectronic memristors including traditional oxides [27], 2D materials [28], organic materials [29], and perovskites [30].

Hereby, we present a novel algorithmic approach for multiclass classification tasks through splitting the problem into binary subtasks while using optoelectronics memristors as synapses. Our approach leverages the core fundamentals from the OvO and the OvR classification strategies towards developing a novel Outcome-Driven One-vs-One (ODOvO) approach. The light modulation of synaptic weights, fed in our algorithm from experimental data [13, 26, 31], is a key enabling parameter that permits classification without modifying further applied electrical biases. In general, classification (not specifically binary) implemented through light modulation of resistance states would require extra multiple iterations at different light illumination amplitudes while keeping electrical biases constant allowing from one hand reduced hardware requirements however extending the time needed per classification step. To this end, our novel ODOvO algorithm provides a solution when instead of iterating through all the pairs we search through the N−1 most likely pairs to classify the sample decreasing both the algorithmic complexity and hardware needs. It is shown that ODOvO retains similar accuracies to the conventional OvO classification while requiring even fewer iterations compared to the OvR. As an example, our MNIST dataset classification using the conventional OvO approach yielded accuracy levels of around 63%, whereas the innovative ODOvO yielded accuracy levels of 62.65% with $\frac{N}{2}$ fewer iterations than OvO, and N-1 less iterations in comparison to the OvR that yielded accuracy of 56.15%.

Overall, our approach based on light modulation of optoelectronic memristors resistance state requires at least a 10X less synapses (only 196 synapses are used) while reducing the total classification time. Consequently, our approach constitutes a feasible solution for neural networks where key priorities are the minimum energy consumption i.e., small iterations number, fast execution, and the low hardware requirements that allow experimental verification. For simple datasets like the MNIST, our binary-classifiers-based algorithms can be used in a fast and efficient way offering the potential for experimental implementation of multi-class classification without the need of hidden layers or convolutional layers.

2 Optoelectronic perovskite memristors in neuromorphic computing

The mixed ionic-electronic conductivity of perovskites renders them suitable for resistive switching memory applications [32]. Perovskite-based memristors have been demonstrated exhibiting a large ON/OFF ratio [33, 34], fast switching speed [35], and good retention [36]. Perovskite memristors have been successfully used for developing crossbar arrays [37], performing logic operations [38], artificial synapses [8], and neural networks [39]. Furthermore, their light-tunable resistance enables the design of photonic perovskite devices that perform logic operations [40] and are used as artificial optoelectronic synapses [41]. The solution-based processing of perovskites enables the use of printing techniques for device fabrication on flexible substrates [42], reducing the complexity and manufacturing cost compared to other technologies such as oxide-based memristors, thus opening the path for flexible processing engines to be integrated in mobile accelerators for wearables IoT systems.

Perovskite memristors operate by either forming conductive filaments between the top and bottom electrodes, or by charge-trapping processes at the interfaces that induce corresponding Schottky barriers [43, 44] allowing the system to transit from a low resistance state (LRS) to a high resistance state (HRS). In the filament-based operation mode, the conductive filament is formed either by active metal cations or by ion migration of mobile species (mainly iodine vacancies (V_I), since they possess the lowest activation energy in the system [45]). Light illumination in perovskite memory devices has reported to cause a Schottky-barrier modification [46] or a filament annihilation [47], leading thus to resistance modulation. Light illumination can alter the ON/OFF ratio of the device during the endurance test, as light causes a controllable modulation of either LRS or HRS, or both states, resulting in a slight reduction of the ON/OFF ratio in many studies [46]. Additionally, the state retention time has been reported not to be affected by light. It is possible that under illumination, some modulation might occur at the LRS and HRS during the first seconds of the measurement, which this process does not affect the retention time of the device compared to measurements taken under dark [48]. The intrinsic conduction mechanism being either filamentary or interface is also affecting how resistance is modulated under light illumination. In devices operating with filaments, light-assisted recombination of ions and vacancies occurs, which causes resistance enhancement under illumination [48]. Overall, the resistance modulation by light illumination in optoelectronic memristors is not expected to cause further variability issues, than these reported in conventional memristors. Ye et al. introduced a lead-free $Cs_2AgBiBr_6$ perovskite memory in an ITO/$Cs_2AgBiBr_6$/PMMA/Ag structure. The device showed a resistance increase under UV light illumination, while being in the LRS, which is attributed to the annihilation of Br vacancies. An optically controlled logic gate and artificial neuromorphic visual system was demonstrated [49].

The structure of the perovskite memristive device used for the experimental data of the current study is depicted in Fig. 1a. It consists of the material stack ITO/PTAA/Perovskite/PCBM/BCP/Ag. All layers are solution-processed and deposited by spin coating except the top electrode, Ag (100 nm), which is thermally evaporated. The perovskite layer is based on a four-cation mixture of Rb, Cs, FA, and MA, abbreviated as RbCsFAMA. More details about the experimental procedures can be found in previous works of the authors [26, 31, 50–52]. The commercially available platform ARKEO (Cicci Research s.r.l.) is used for current–voltage (I–V) measurements. The voltage is swept from + 1 to − 1.2 V, and a compliance current of 10 mA is used to protect the device. All measurements are performed in ambient air under 25 °C. Figure 1b shows 20 representative I-V curves of a typical memristive device. As it is evident, the device shows stable bipolar switching behaviour and operates at low voltage bias (< 1 V). The average SET voltage is 0.13 ± 0.04 V, and the average RESET voltage is − 0.75 ± 0.04 V. The ON/OFF ratio is ~ 10^3. The device operates based on the formation and rupture of a conductive filament between the top and the bottom electrode. According to our previous work, the device operates by the formation and rupture of a conductive filament based on metallic electrode (Ag) and by halide vacancies (I and Br) [36]. The device exhibits an inverse photoconductivity behaviour, thus the resistance increases upon illumination because of a light-enhanced halides recombination process [45], which ruptures the conductive filament [53]. The same effect has also been confirmed in other halide perovskite memory devices [54, 55]. Hence, the device gradually transits to HRS, and the

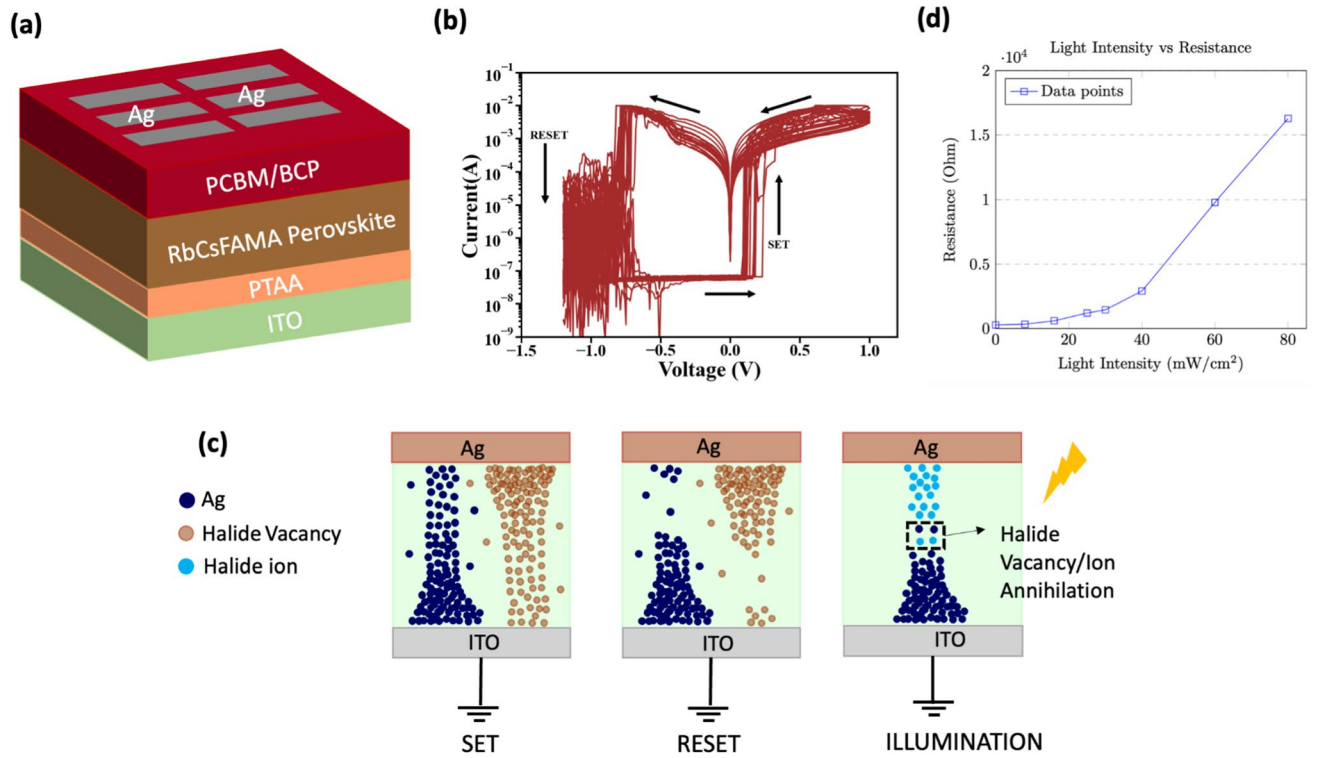

Fig. 1 **a** Cross-sectional view of the halide perovskite memory device, showing layers from ITO to Ag electrode. **b** 20 I–V curves illustrating the low-power, stable bipolar switching behaviour of the device. **c** Schematic diagram showing the formation and rupture of the conductive filament in the device during operation and under illumination. **d** Almost Linear Correlation of light intensity vs Resistance in perovskite based optoelectronic memristors as extracted by experiment [13, 26],

transition can be tuned by controlling the illumination intensity. Figure 1d depicts an almost linear correlation of light intensity with memristors resistance, for specific illumination intensity range (~40 mW/cm^2–80 mW/cm^2) as extracted by experimental perovskite optoelectronic memristors. The formation and rupture of the conductive filament during SET and RESET, as well as the filament rupture under illumination, are illustrated in Fig. 1c. Table 1 shows a comparison between conventional oxide-based and perovskite memristors. It is noted that perovskite devices with high ON/OFF ratios operating at low electric fields can be realised, with good retention properties approaching the performance of oxide-based devices. However, the cycling endurance of these devices is inferior compared to regular oxide systems. Variability is an issue that hinders the performance of perovskite memristive devices as well.

Herein, we used the experimental dependence of memristors resistance on light illumination reported in Fig. 1d [13, 26, 31]. Owing to this light-modulation feature, we can apply various binary classification algorithms such as OvO, OvR

Table 1 Comparative key performance indicators of Perovskite-Based and Regular Oxide-Based Memristors

Material	VSET/VRESET (V)	ON/OFF Ratio	Endurance (Cycles)	Retention (s)	Refs.
ZnO	0.3/– 0.3	10^6	3×10^4	5×10^4	[56]
TiO2	1.5/– 2.8	10^2	10^7	10^5	[57]
CuxO	~ 2/– 3	10^3	1.2×10^4	2×10^4	[58]
TaOx	~ – 1/~ 2	10^2	10^{12}	$> 10^4$	[59]
HfO2/BiFeO3	~1.5/– 2.0	10^4	10^8	10^4	[60]
CH3NH3PbI3	0.85/– 1.4	10^3	3.5×10^2	10^4	[61]
α-FAPbI3	– 2.4/2.3	10^2	1.2×10^3	10^3	[62]
CH3NH3PbI3-xClx	1.1/– 1.65	1.9×10^9	1.6×10^2	2×10^3	[33]
Cs0.06FA0.78MA0.16 Pb(I0.92Br0.08)3	4/– 4	10^2	10^3	10^5	[63]
CsBi3I10	– 1.7/0.9	10^3	1.5×10^2	10^4	[64]

and our proposed ODOvO and proceed to classification by tuning purely the memristive state by light intensity. This extra degree of freedom allows one single crossbar array to classify the problem using the electrical bias as inputs, while being able to be adjusted further to other synaptic weights by using variable light intensities.

3 Background and methodology for OvO, OvR, and the novel Output-Driven OvO

This concept of binary classifiers has been already addressed in the field of pattern recognition and specifically in neural networks using the OvO [65] and OvR [66] classification strategies, which split the problems into binary classifications that combined assist in finding the solution of the problem. These approaches can be applied effectively in the classifications of multiclass complex problems where the easiness of the approach and hardware simplicity are priorities despite their lower accuracy compared to complex classification algorithms. We take advantage of the light modulation in perovskite optoelectronic memristors and build corresponding neural networks implementing various algorithmic approaches for simplified multiclass classifications based on binary classifiers. The three binary classification algorithms (OvO, OvR, ODOvO) when applied to conventional memristors that do not allow optoelectronic control will require higher number of synapses by a factor of 10X to achieve the same accuracy with the same number of iterations. Optoelectronic memristors light tunability is therefore the key enabling parameter to implement all binary classifiers (OvO, OvR, ODOvO) without applying new electrical biases after each iteration, a process that consumes power and also adds time delays [67]. Consequently, using optoelectronic memristors gives the advantage of splitting up big computation tasks or big classifications for pattern recognition into many simpler binary classifications which wouldn't make sense for traditional memristors. Optoelectronic memristors therefore can be used to reduce the hardware complexity required for neural network applications [68, 69].

It is noted that a specific local photo-addressing hardware is required for the experimental realisation of our concept. There are available techniques to apply locally varying light intensity so be able to set training weights through light modulation. One option is to use laser pulses to scan across the various memristive nodes and control light intensity locally [70–72]. Alternatively, an array of LEDs can be developed on top of the memristors array controlling the light intensity on each memristor. A third option could be the integration of electrochromic pixels on top of each memristive node [73],where in this case one constant light source is needed and light modulation could be achieved locally by tuning the light transparency of the electrochromic pixels through electrical pulses application. The experimental realisation of the local light control could add some extra hardware complexity, however, resolving this extrinsic to the memristive nodes hardware complexity is out of the scope of the current study.

Both OvO and OvR could have a key advantage when implemented using optoelectronic memristors in real-life problems. An example of OvO and OvR in action for classifying a 10 multiclass problem is depicted in Fig. 2. In the OvO, each complex multiclass problem is split into all the $\frac{[N(N-1)]}{2}$ [65] pairs of classifiers that are available for this classification. This allows the classifiers to scan across all the available pairs and distinguish the complex relationships between the classes, thus allowing a more accurate inference for the classification. This process is however computationally expensive requiring $\frac{[N(N-1)]}{2}$ iterations of all the trained weights to classify each sample of the problem. For multiclass problems using OvO, addressing the light modulations for all the trained classifiers would require significant time. Since a single hardware architecture should handle the classification problem, more effective ways towards reducing the time of execution per each sample should be identified. To this end, a more effective approach to classifying the problem in binary subtasks is the OvR. This approach has the benefit of requiring less training steps since only *N* classifiers should be trained for all the cases mentioned, while a larger range of training per each classifier can be used, *whereasN* is the number of classes in the dataset. In this approach, each class is trained against all the other classes; therefore, each classifier can distinguish the class we train it on and keep all the rest classes as one class. Following this method, *N* iterations should be applied after the training phase based on all the available classes, and then, the class that resembles the highest probability is the one selected to classify the problem. This process however has issues in cases of having similar classes because this approach cannot capture in detail the relationships and differences of the classes. This is especially the case when the data are resized to be utilised in smaller harwares, where some classes might be overlapping. Overall, this approach can capture enough details for most applications when implemented with optoelectronic memristors.

To overcome the above mentioned issues, we hereby propose another classification algorithm based on a modified version of the OvO approach, while being able to achieve classification at sufficient accuracy with as low as possible number of iterations per classification. The proposed solution, termed as Outcome Driven One vs One (ODOvO), utilises the core basics of OvO in which each pair of classes is separately split leading to $\frac{[N(N-1)]}{2}$ trained classifiers. An example

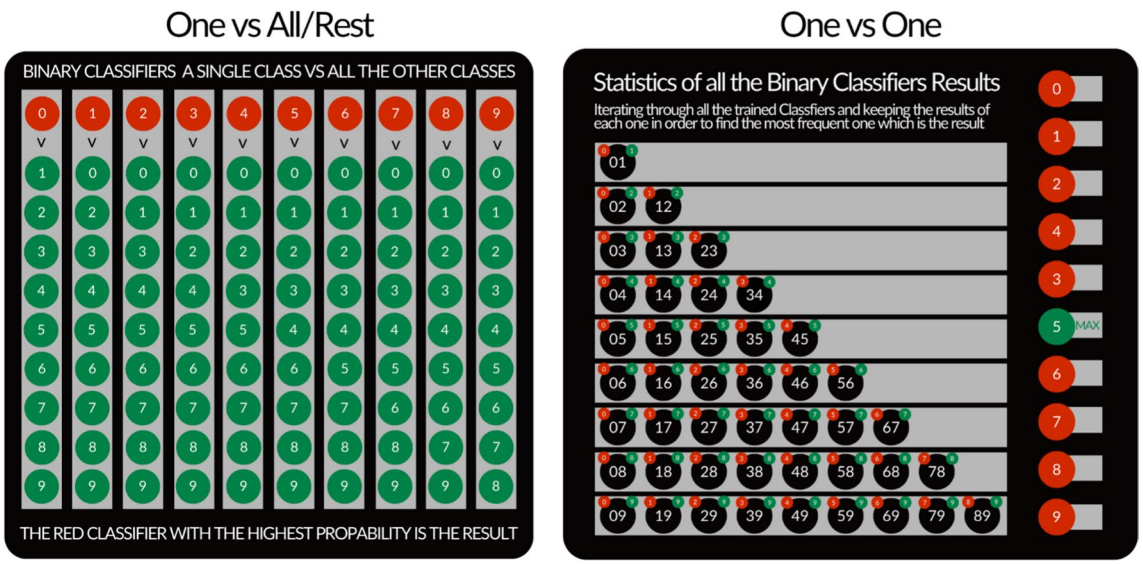

Fig. 2 Example of One vs One and One Vs All in action for classifying in a 10 multiclass problem. We can see clearly that the One vs All classifier trains each class independently against all the rest available as one ending with ten classifiers for the MNIST dataset. On the right, we can see the classifier is creating individual pairs among all the possible combinations of numbers available and taking statistics on how many times each individual number has been classified

of the ODOvO in action for classifying the fifth class in a 10 multiclass problem is depicted in Fig. 3. Following ODOvO on the other hand, a dynamic approach is implemented to classify the sample thus N-1 iterations are needed, instead of the $\frac{[N(N-1)]}{2}$ iterations needed for standard OvO classifications. For architectures based on optoelectronic memristor this novel approach can have a huge advantage since it allows to reduce the required iterations of light modulations that can have a significant impact on the total time needed to classify the problem. To achieve an ODOvO classification, we initially train the classifiers similarly to the OvO approach, but adding to this, the outcome of the first pair of classes classification is used as input for the next classifier. Specifically, based on the outcome of the first class that is either 0 or 1, we accordingly continue with the next trained weights of the classifiers. This means that if the result of the first classifier remains "zero," meaning the first class of the problem seems to be the most likely result, we then move to the next trained classifier of the first class (move vertically from top to bottom in Fig. 3). If the outcome is "zero," meaning the second class is more likely to resemble the sample, we move on the trained weights of the classifier that most closely resembles the class from the previous iteration (move horizontally from left to right in Fig. 3). This class will be compared with the next

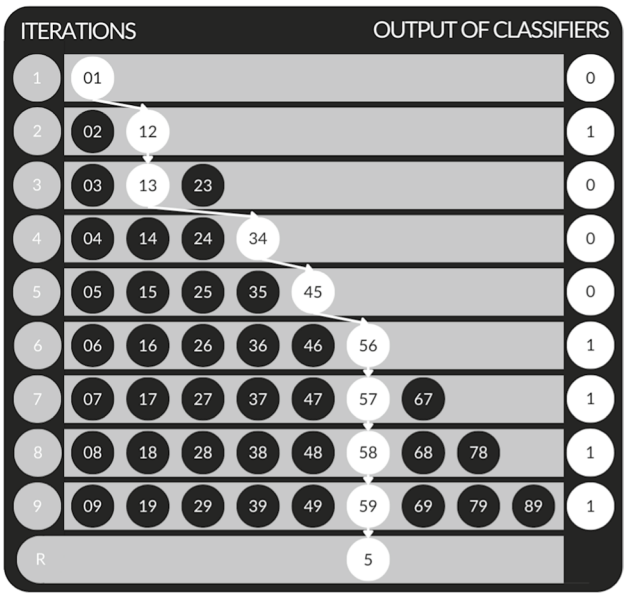

Fig. 3 Example of the Outcome-Driven One vs One (ODOvO) in action for classifying the fifth class in a 10 multiclass problem. We note that the pairs of Binary classifiers of the sample are being driven by the result of each iteration to achieve the final classification

available class. Therefore, based on the outcome of each pair classification, we move on to the next pair that would be the most likely for our classification problem.

Overall, this approach makes iterations across all the classes but in the form of the most likely pairs achieving accuracies close to OvR, while reducing the number of iterations needed for the classification from $\frac{[N(N-1)]}{2}$ of the OvO down to $N-1$That is even less than the OvR approach.

The pseudocode for this classification's algorithm is listed below.

Algorithm 1 Outcome Driven One vs One (ODOvO)

```
procedure GET WEIGHT MAP(current map, outcome, max classes)
    if current map is None then
        return "weights01"
    end if
    Let digit1 = first digit extracted from current map
    Let digit2 = second digit extracted from current map
    if outcome equals 1 then
        digit2 = digit2 + 1
    else
        digit1 = digit2
        digit2 = digit1 + 1
    end if
    if digit2 equals max classes then
        return None
    end if
    Let next map = "weights" concatenated with digit1 and digit2
    return next map

end procedure
```

Algorithm 2 Final Classification

```
procedure CLASSIFY FINAL MAP(current map, outcome)
    Let final digit = first digit if outcome equals 1 else second digit from current map
    Let predicted label = final digit
    return predicted label

end procedure
```

Now let's try an example using the above pseudocode. Let's assume that the sample we are trying to classify is the number "5" class (see Fig. 3). The first classifier for this will be the pair of "0" and "1" classes, where this comparison will

result in zero that means it has closer relation to the class "1" (iteration 1 in Fig. 3). Now it will adjust the weights to classify the class "1" and "2" resulting in the outcome of one, which means this sample has closer relation to the class "1" (iteration 2). It now adjusts the weights for the class "1" and "3" which results in the outcome of zero (iteration 3) leading to swapping the second class to become the first and the new second class to be the next digit of the new first class, therefore, classifying for "3" and "4" (move vertically from iteration 3 to 4 in Fig. 3). This process will continue based on the outcome that is still zero (iteration 4), adjusting the weights for classification to identify whether the class is "4" or "5", which still results in zero (iteration 5), which will result, in changing to the classes pair of "5" and "6". After that, this classifier results into one (iteration 6) changing the weights to classify the pair of "5" and "7", which also results into one (iteration 7) therefore also changing the weights to "5" and "8", which then also results to one (iteration 8) leading the final weights loaded to the classifier being the classes of "5" and "9" which will classify the final result of the sample based on the result of those two classes. This outputs also "1" (iteration 9) which will categorise this sample to the class number "5" correctly (Result). Above we can see the visual interpretation of the abovementioned example for classification.

This approach, similarly, to the previous ones, possesses big advantages for the implementation of neural networks using optoelectronic memristors since they can harness the light modulation of memristors conductance to adjust the weights and classify multiclass complex problems with simple binary classification architectures. It's important to note that this algorithm might not perform equally well in cases where the first classes in the iteration are not very separable, but for examples where the time of execution is the key parameter would be an ideal solution. In applications where optoelectronic memristors are integrated, the iterations are handled as hardware changes in response to light intensity thus offering the ability to raise the accuracy while requiring fewer iterations. For some specific applications or datasets, the use of the traditional OvO or OvR might perform better than ODOvO thus it is important to test all the algorithms for various use-case scenarios. The ODOvO approach is an intermediate step between the two already established algorithms for binary classifications with the goal of reducing the iterations needed to classify the problem. Its application would result to fewer light modulations needed on optoelectronic memristors while retaining accuracy levels comparable to the OvO approach and reducing the iterations needed for classification by a factor of $\frac{N}{2}$.

4 Proposed architectures for performance evaluation and benchmarking

The proposed algorithmic architectures employ a cascading series of binary classifiers based on Feedforward Neural Networks (FNNs). Each of the classifiers is a single-layer NN with sigmoid activation function [74] to ensure that the synaptic weights are positive in agreement with the experiment where the imported conductance values of optoelectronic memristors are always positive. The weights and biases of the FNNs are adjusted and learned through a basic gradient descent algorithm based on the error of the network output and the actual labels. Binary classifiers are used to split those multiclass problems by implementing the OvO, the OvR, and the ODOvO approaches. This approach can be implemented with optoelectronic memristors as cascading classifiers by directly modulating the light intensity of the interconnected memristors, which alters the conductivity of each memristor almost instantaneously. In this work, we utilised the MNIST Dataset (Modified National Institute of Standards and Technology database) [75] due to its inherent nature of classifying numbers as well as its popularity and wide use for benchmarking. We trained the dataset through individual pairs training focusing on only two specific numbers using a rather simple architecture for the FNN resulting in 45 pairs. This results in 45 different classifiers for the case of OvO and the ODOvO, and 10 classifiers for the OvR approach.

Aiming at developing classification architectures that can be realised experimentally we tried to reduce the hardware requirements as much as possible. To this end, we pre-processed the MNIST [75] dataset from the original 28×28 size to 14×14 size. This scaling down to only 196 synapses (thus 196 memristors), although could limit the accuracy of the classification algorithm, can be experimentally realised and allow the hardware benchmarking of the proposed algorithms. The images of Fig. 4 are encoded applying a threshold to the pixel intensity that serves as input for the NN. We can see in Fig. 5 the process it takes on the crossbar for the actual classification process. The electrical inputs are the inputs of the classifying sample and with the iterations of the different trained light intensities we can come to the final solution. It's crucial to mention that the same hardware synapses are used for all the 9, 10 or 45 iterations, depending on the classification approach, in order to achieve the final classification of the sample. In all cases, the only adjustments in synaptic weights of the FNN are implemented through modulation of light intensities.

All three approaches showed promising results when used to classify the same 2000 images using the same architectures and epochs for the training of the MNIST Dataset (Table 2). The OvO required 45 iterations of weights per

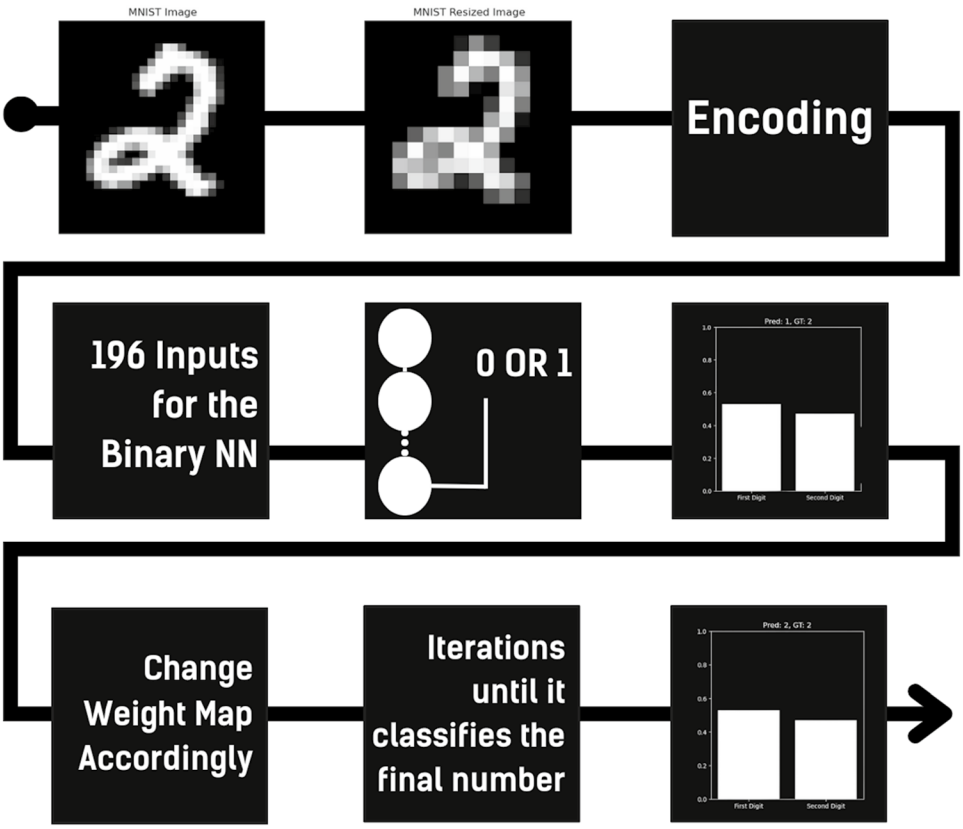

Fig. 4 Structure of the Neural Network Architecture. The sample is received as an input, then resized to a smaller dimension to be encoded and classified on the Binary classifiers of the OvO, OvR and ODOvO

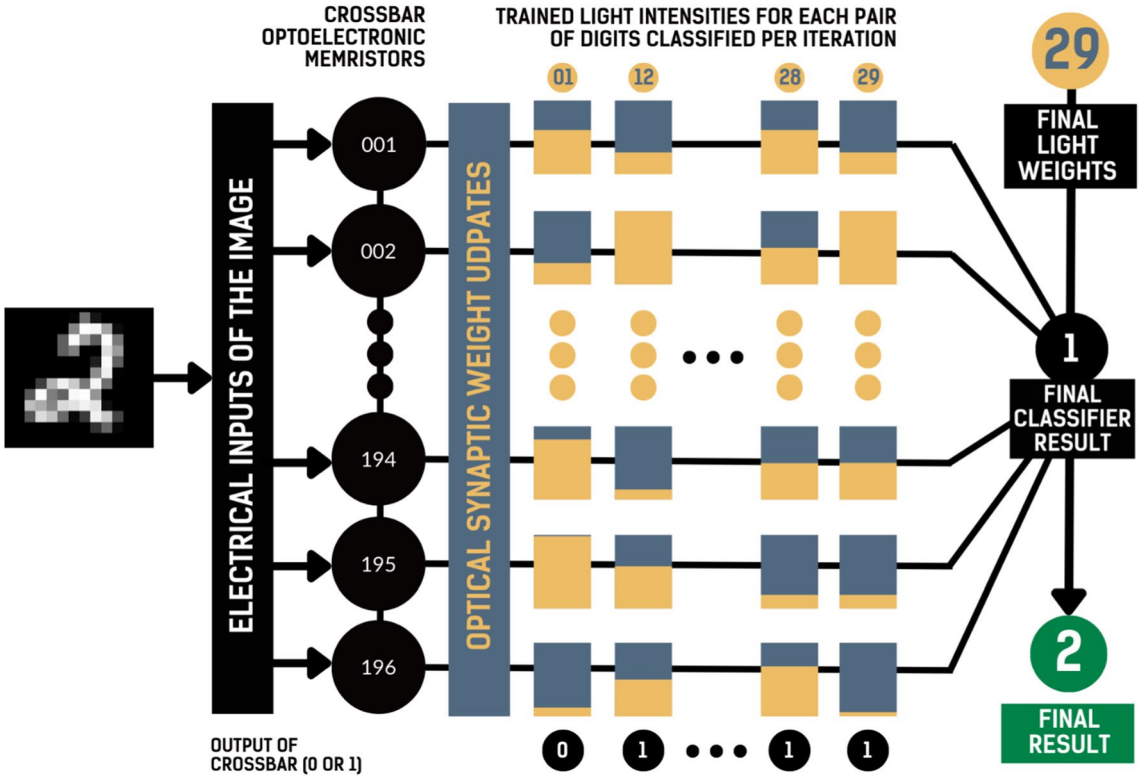

Fig. 5 Proposed architecture with the different light intensities applied in the devices until the final classification

Table 2 Different algorithms utilised for binary classifications of the Optoelectronic Memristor Neural Networks

ALGORITHMS	Iterations	Trained weights	Accuracy (%)	Iterations	Hardware synapses with light	Hardware synapses without light
ODOvO	9	45	62.65	(N−1)	196	8820
OvO	45	45	63.2	[N(N−1)]/2	196	8820
OvR	10	10	56.15	N	196	1960

classification and was the most accurate with accuracy levels of 63.2%. The novel approach of ODOvO required only 9 iterations of weights per classification and had very similar accuracy levels results with the OvO (62.65%) while requiring 5 times fewer iterations of weights and therefore 5 times fewer light modulations implemented on the memristors. Finally, the OvR required 10 iterations of weights per classification (like the ODOvO), while only 9 iterations were needed achieving accuracy levels of 56.15%. More details and extended results can be found in the supplemental information. The use of all these approaches offers major benefits as we can classify a 10-class classification problem that would normally require more complex architectures by harnessing the properties of the light-triggered memristors. Additionally, the proposed ODOvO algorithm reduces the number of iterations needed by a factor of $\frac{N}{2}$, and thus the number of light modulations needed per successful iterations, without losing on accuracy in comparison to standard algorithms such as the OvO.

The innovative ODOvO algorithm and the use of binary classifications in general, such as OvO and OvR for multiclass classifications, combined with the use of optoelectronic memristors constitute an advancement compared to conventional computation architectures. These approaches could also be achieved in Spiking Neural Networks (SNN), although this implementation raises the complexity [76]. We additionally implemented the OvO approach using Snntorch [77] with Leaky-Integrate and fire [78] as a proof of concept in a similar architecture to the originally proposed architecture (see supplementary information for further information).

5 Conclusion

We explored the theoretical usage of binary classification algorithms such as OvO and OvR to address the hardware limitations of experimental neuromorphic crossbars targeting models' verifications in real-life scenarios. Furthermore, we proposed an innovative variation of OvO, termed as ODOvO that retains satisfactory accuracy levels while reducing the required iterations by a factor $\frac{N}{2}$. These binary classification architectures take advantage of the light modulation of the resistance states achieved in optoelectronic memristors to perform multiple binary classifications within the same crossbar device, simplifying the problem of multiclass classification and making it a viable solution towards less hardware-intensive configurations requiring at least a 10X less synapses compared to conventional memristors. We used the MNIST [75] dataset as a testbed to validate this approach, demonstrating that the use of optoelectronic memristors in NN applications could reduce energy consumption and hardware complexity. This approach provides a foundation for further research for tailored algorithms targeting neuromorphic computing hardware, showing potential for efficiently addressing complex computational tasks such as multiclass classification.

Acknowledgements The work has been supported by the European Union's Horizon 2020 research and Innovation program under project EMERGE. The EMERGE project has received funding under Grant Agreement No. 101008701.

Author contributions GP wrote the main manuscript text, with specifically contributing to conceptualization, formal analysis, and data curation with inputs from EK and KR. ML focused on data curation. EK and KR provided review editing and supervision. All authors reviewed the manuscript.

Data availability The authors declare that the data supporting the findings of this study are available within the paper, its supplementary information files, and their GitHub repository link listed above.

Code availability The code is available at https://github.com/psaltakis/ODOvA.

Declarations

Competing interests The authors declare no competing interests.

References

1. Venianaki M, Salvetti O, de Bree E, Maris T, Karantanas A, Kontopodis E, Nikiforaki K, Marias K. Pattern recognition and pharmacokinetic methods on DCE-MRI data for tumor hypoxia mapping in sarcoma. Multimed Tools Appl. 2018;77:9417–39. https://doi.org/10.1007/s11042-017-5046-6.
2. Mori S, Suen CY, Yamamoto K. Historical review of OCR research and development. Proc IEEE. 1992;80:1029–58. https://doi.org/10.1109/5.156468.
3. Vijaya Kumar BVK, Savvides M, Xie C. Correlation pattern recognition for face recognition. Proc IEEE. 2006;94:1963–76. https://doi.org/10.1109/JPROC.2006.884094.
4. Jain AK. Biometric recognition: overview and recent advances. In: Rueda L, Mery D, Kittler J, editors. Progress in pattern recognition, image analysis and applications. Berlin, Heidelberg: Springer; 2007. p. 13–9. https://doi.org/10.1007/978-3-540-76725-1_2.
5. Mehonic A, Kenyon AJ. Brain-inspired computing needs a master plan. Nature. 2022;604:255–60. https://doi.org/10.1038/s41586-021-04362-w.
6. Mehonic A, Sebastian A, Rajendran B, Simeone O, Vasilaki E, Kenyon AJ. Memristors—from in-memory computing, deep learning acceleration, and spiking neural networks to the future of neuromorphic and bio-inspired computing. Adv Intell Syst. 2020;2:2000085. https://doi.org/10.1002/aisy.202000085.
7. Emboras A, Alabastri A, Lehmann P, Portner K, Weilenmann C, Ma P, Cheng B, Lewerenz M, Passerini E, Koch U, Aeschlimann J, Ducry F, Leuthold J, Luisier M. Opto-electronic memristors: prospects and challenges in neuromorphic computing. Appl Phys Lett. 2020;117:230502. https://doi.org/10.1063/5.0028539.
8. Liu J, Gong J, Wei H, Li Y, Wu H, Jiang C, Li Y, Xu W. A bioinspired flexible neuromuscular system based thermal-annealing-free perovskite with passivation. Nat Commun. 2022;13:7427. https://doi.org/10.1038/s41467-022-35092-w.
9. Venkatesan T, Williams S. Brain inspired electronics. Appl Phys Rev. 2022;9:010401. https://doi.org/10.1063/5.0078798.
10. Gerasimov JY, Zhao D, Sultana A, Abrahamsson T, Han S, Bliman D, Tu D, Simon DT, Olsson R, Crispin X, Berggren M, Fabiano S. A biomimetic evolvable organic electrochemical transistor. Adv Electron Mater. 2021;7:2001126. https://doi.org/10.1002/aelm.202001126.
11. van de Burgt Y, Gkoupidenis P. Organic materials and devices for brain-inspired computing: from artificial implementation to biophysical realism. MRS Bull. 2020;45:631–40. https://doi.org/10.1557/mrs.2020.194.
12. Sheridan P, Ma W, Lu W Pattern recognition with memristor networks. In: 2014 IEEE International Symposium on Circuits and Systems (ISCAS). 2014. P. 1078–81. https://doi.org/10.1109/ISCAS.2014.6865326
13. Rogdakis K, Loizos M, Viskadouros G, Kymakis E. Memristive perovskite solar cells towards parallel solar energy harvesting and processing-in-memory computing. Mater Adv. 2022;3:7002–14. https://doi.org/10.1039/D2MA00402J.
14. Zidan MA, Strachan JP, Lu WD. The future of electronics based on memristive systems. Nat Electron. 2018;1:22–9. https://doi.org/10.1038/s41928-017-0006-8.
15. Park H-L, Lee Y, Kim N, Seo D-G, Go G-T, Lee T-W. Flexible neuromorphic electronics for computing, soft robotics, and neuroprosthetics. Adv Mater. 2020;32:1903558. https://doi.org/10.1002/adma.201903558.
16. Lanza M, Sebastian A, Lu WD, Le Gallo M, Chang M-F, Akinwande D, Puglisi FM, Alshareef HN, Liu M, Roldan JB. Memristive technologies for data storage, computation, encryption, and radio-frequency communication. Science. 2022;376:eabj9979. https://doi.org/10.1126/science.abj9979.
17. Yu S. Neuro-inspired computing using resistive synaptic devices. Cham: Springer International Publishing; 2017. https://doi.org/10.1007/978-3-319-54313-0.
18. Rogdakis K, Psaltakis G, Fagas G, Quinn A, Martins R, Kymakis E. Hybrid chips to enable a sustainable internet of things technology: opportunities and challenges. Discov Mater. 2024;4:4. https://doi.org/10.1007/s43939-024-00074-w.
19. Zhao X, Xu H, Wang Z, Lin Y, Liu Y. Memristors with organic-inorganic halide perovskites. InfoMat. 2019;1:183–210. https://doi.org/10.1002/inf2.12012.
20. Wang Y, Yin L, Huang W, Li Y, Huang S, Zhu Y, Yang D, Pi X. Optoelectronic synaptic devices for neuromorphic computing. Adv Intell Syst. 2021;3:2000099. https://doi.org/10.1002/aisy.202000099.
21. Zhou F, Zhou Z, Chen J, Choy TH, Wang J, Zhang N, Lin Z, Yu S, Kang J, Wong H-SP, Chai Y. Optoelectronic resistive random access memory for neuromorphic vision sensors. Nat Nanotechnol. 2019;14:776–82. https://doi.org/10.1038/s41565-019-0501-3.
22. Wang W, Yin F, Niu H, Li Y, Kim ES, Kim NY. Tantalum pentoxide (Ta2O5 and Ta2O5-x)-based memristor for photonic in-memory computing application. Nano Energy. 2023;106:108072. https://doi.org/10.1016/j.nanoen.2022.108072.
23. Hu L, Yang J, Wang J, Cheng P, Chua LO, Zhuge F. All-optically controlled memristor for optoelectronic neuromorphic computing. Adv Funct Mater. 2021;31:2005582. https://doi.org/10.1002/adfm.202005582.
24. Pereira ME, Martins R, Fortunato E, Barquinha P, Kiazadeh A. Recent progress in optoelectronic memristors for neuromorphic and in-memory computation. Neuromorphic Comput Eng. 2023;3:022002. https://doi.org/10.1088/2634-4386/acd4e2.
25. Chen Z-L, Xiao Y, Huang W-Y, Jiang Y-P, Liu Q-X, Tang X-G. In-sensor reservoir computing based on optoelectronic synaptic devices. Appl Phys Lett. 2023;123:100501. https://doi.org/10.1063/5.0160599.
26. Loizos M, Rogdakis K, Kymakis E. An electronic synaptic memory device based on four-cation mixed halide perovskite. Discov Mater. 2022;2:11. https://doi.org/10.1007/s43939-022-00032-4.

27. Hassan MY, Ang DS. On-demand visible-light sensing with optical memory capabilities based on an electrical-breakdown-triggered negative photoconductivity effect in the ubiquitous transparent hafnia. ACS Appl Mater Interfaces. 2019;11:42339–48. https://doi.org/10.1021/acsami.9b13552.
28. Liu C, Zou X, Wu M-C, Wang Y, Lv Y, Duan X, Zhang S, Liu X, Wu W-W, Hu W, Fan Z, Liao L. Polarization-resolved broadband MoS2/black phosphorus/MoS2 optoelectronic memory with ultralong retention time and ultrahigh switching ratio. Adv Funct Mater. 2021;31:2100781. https://doi.org/10.1002/adfm.202100781.
29. Sun J, Chen Q, Fan F, Zhang Z, Han T, He Z, Wu Z, Yu Z, Gao P, Chen D, Zhang B, Liu G. A dual-mode organic memristor for coordinated visual perceptive computing. Fundam Res. 2022. https://doi.org/10.1016/j.fmre.2022.06.022.
30. Xiao X, Hu J, Tang S, Yan K, Gao B, Chen H, Zou D. Recent advances in halide perovskite memristors: materials, structures, mechanisms, and applications. Adv Mater Technol. 2020;5:1900914. https://doi.org/10.1002/admt.201900914.
31. Rogdakis K, Chatzimanolis K, Psaltakis G, Tzoganakis N, Tsikritzis D, Anthopoulos TD, Kymakis E. Mixed-halide perovskite memristors with gate-tunable functions operating at low-switching electric fields. Adv Electron Mater. 2023;9:2300424. https://doi.org/10.1002/aelm.202300424.
32. Futscher MH, Milić JV. Mixed conductivity of hybrid halide perovskites: emerging opportunities and challenges. Front Energy Res. 2021. https://doi.org/10.3389/fenrg.2021.629074.
33. Yan K, Peng M, Yu X, Cai X, Chen S, Hu H, Chen B, Gao X, Dong B, Zou D. High-performance perovskite memristor based on methyl ammonium lead halides. J Mater Chem C. 2016;4:1375–81. https://doi.org/10.1039/C6TC00141F.
34. Kim H, Choi M-J, Suh JM, Han JS, Kim SG, Le QV, Kim SY, Jang HW. Quasi-2D halide perovskites for resistive switching devices with ON/OFF ratios above 109. NPG Asia Mater. 2020;12:1–11. https://doi.org/10.1038/s41427-020-0202-2.
35. Hwang B, Lee J-S. A strategy to design high-density nanoscale devices utilizing vapor deposition of metal halide perovskite materials. Adv Mater. 2017;29:1701048. https://doi.org/10.1002/adma.201701048.
36. Sun Y, Tai M, Song C, Wang Z, Yin J, Li F, Wu H, Zeng F, Lin H, Pan F. Competition between metallic and vacancy defect conductive filaments in a CH3NH3PbI3-based memory device. J Phys Chem C. 2018;122:6431–6. https://doi.org/10.1021/acs.jpcc.7b12817.
37. Kang K, Ahn H, Song Y, Lee W, Kim J, Kim Y, Yoo D, Lee T. High-performance solution-processed organo-metal halide perovskite unipolar resistive memory devices in a cross-bar array structure. Adv Mater. 2019;31:1804841. https://doi.org/10.1002/adma.201804841.
38. Sun Y, Wen D. Logic function and random number generator build based on perovskite resistive switching memory and performance conversion via flexible bending. ACS Appl Electron Mater. 2020;2:618–25. https://doi.org/10.1021/acsaelm.9b00836.
39. John RA, Shah N, Vishwanath SK, Ng SE, Febriansyah B, Jagadeeswararao M, Chang C-H, Basu A, Mathews N. Halide perovskite memristors as flexible and reconfigurable physical unclonable functions. Nat Commun. 2021;12:3681. https://doi.org/10.1038/s41467-021-24057-0.
40. Lin G, Lin Y, Cui R, Huang H, Guo X, Li C, Dong J, Guo X, Sun B. An organic–inorganic hybrid perovskite logic gate for better computing. J Mater Chem C. 2015;3:10793–8. https://doi.org/10.1039/C5TC02270C.
41. Hao D, Zhang J, Dai S, Zhang J, Huang J. Perovskite/organic semiconductor-based photonic synaptic transistor for artificial visual system. ACS Appl Mater Interfaces. 2020;12:39487–95. https://doi.org/10.1021/acsami.0c10851.
42. Lin Q, Hu W, Zang Z, Zhou M, Du J, Wang M, Han S, Tang X. Transient resistive switching memory of CsPbBr 3 thin films. Adv Electron Mater. 2018;4:1700596. https://doi.org/10.1002/aelm.201700596.
43. Liu Y, Li F, Chen Z, Guo T, Wu C, Kim TW. Resistive switching memory based on organic/inorganic hybrid perovskite materials. Vacuum. 2016;130:109–12. https://doi.org/10.1016/j.vacuum.2016.05.010.
44. Xu Z, Liu Z, Huang Y, Zheng G, Chen Q, Zhou H. To probe the performance of perovskite memory devices: defects property and hysteresis. J Mater Chem C. 2017;5:5810–7. https://doi.org/10.1039/C7TC00266A.
45. Eames C, Frost JM, Barnes PRF, O'Regan BC, Walsh A, Islam MS. Ionic transport in hybrid lead iodide perovskite solar cells. Nat Commun. 2015;6:7497. https://doi.org/10.1038/ncomms8497.
46. Guan X, Hu W, Haque MA, Wei N, Liu Z, Chen A, Wu T. Light-responsive ion-redistribution-induced resistive switching in hybrid perovskite Schottky junctions. Adv Funct Mater. 2018;28:1704665. https://doi.org/10.1002/adfm.201704665.
47. Zhu X, Lee J, Lu WD. Iodine vacancy redistribution in organic-inorganic halide perovskite films and resistive switching effects. Adv Mater. 2017;29:1700527. https://doi.org/10.1002/adma.201700527.
48. Sheykhifar Z, Mohseni SM. Highly light-tunable memristors in solution-processed 2D materials/metal composites. Sci Rep. 2022;12:18771. https://doi.org/10.1038/s41598-022-23404-5.
49. Ye H, Liu Z, Sun B, Zhang X, Shi T, Liao G. Optoelectronic resistive memory based on lead-free Cs2AgBiBr 6 double perovskite for artificial self-storage visual sensors. Adv Electron Mater. 2023;9:2200657. https://doi.org/10.1002/aelm.202200657.
50. Tzoganakis N, Feng B, Loizos M, Chatzimanolis K, Krassas M, Tsikritzis D, Zhuang X, Kymakis E. Performance and stability improvement of inverted perovskite solar cells by interface modification of charge transport layers using an azulene-pyridine molecule. Energy Technol. 2023;11:2201017. https://doi.org/10.1002/ente.202201017.
51. Tzoganakis N, Feng B, Loizos M, Krassas M, Tsikritzis D, Zhuang X, Kymakis E. Ultrathin PTAA interlayer in conjunction with azulene derivatives for the fabrication of inverted perovskite solar cells. J Mater Chem C. 2021;9:14709–19. https://doi.org/10.1039/D1TC02726C.
52. Tsikritzis D, Rogdakis K, Chatzimanolis K, Petrović M, Tzoganakis N, Najafi L, Martín-García B, Oropesa-Nuñez R, Bellani S, Castillo AEDR, Prato M, Stylianakis MM, Bonaccorso F, Kymakis E. A two-fold engineering approach based on Bi 2 Te 3 flakes towards efficient and stable inverted perovskite solar cells. Mater Adv. 2020;1:450–62. https://doi.org/10.1039/D0MA00162G.
53. Gu C, Lee J-S. Flexible hybrid organic-inorganic perovskite memory. ACS Nano. 2016;10:5413–8. https://doi.org/10.1021/acsnano.6b01643.
54. Zhu X, Lu WD. Optogenetics-inspired tunable synaptic functions in memristors. ACS Nano. 2018;12:1242–9. https://doi.org/10.1021/acsnano.7b07317.
55. Wang Y, Xiong Y, Sha J, Guo J, Wang H, Qiang Z, Shang Y, Jia R, Sun K, Huang F, Gan X, Wang S. Inverse photoconductivity effect in triple cation organic–inorganic hybrid perovskite memristors with various iodine concentrations, electrodes, and modified layers. J Mater Chem C. 2022;10:1414–20. https://doi.org/10.1039/D1TC04757D.
56. Park Y, Lee J-S. Bifunctional silver-doped ZnO for reliable and stable organic-inorganic hybrid perovskite memory. ACS Appl Mater Interfaces. 2021;13:1021–6. https://doi.org/10.1021/acsami.0c18038.

57. Xue D, Song H, Zhong X, Wang J, Zhao N, Guo H, Cong P. Flexible resistive switching device based on the TiO2 nanorod arrays for non-volatile memory application. J Alloys Compd. 2020;822:153552. https://doi.org/10.1016/j.jallcom.2019.153552.
58. Hsu C-C, Hua S-Y, Zhang X-Z, Jhang W-C, Cheng C-W, Tsai J-E, Wu Y-M, Chien Y-S, Wu W-C. Effects of interfacial oxide layer formed by annealing process on WORM characteristics of Ag/CuxO/SiOx/n+–Si devices. J Alloys Compd. 2022;898:162918. https://doi.org/10.1016/j.jallcom.2021.162918.
59. Lee M-J, Park G-S, Seo DH, Kwon SM, Lee H-J, Kim J-S, Jung M, You C-Y, Lee H, Kim H-G, Pang S-B, Seo S, Hwang H, Park SK. Reliable multivalued conductance states in TaOx memristors through oxygen plasma-assisted electrode deposition with in situ-biased conductance state transmission electron microscopy analysis. ACS Appl Mater Interfaces. 2018;10:29757–65. https://doi.org/10.1021/acsami.8b09046.
60. Liu L, Xiong W, Liu Y, Chen K, Xu Z, Zhou Y, Han J, Ye C, Chen X, Song Z, Zhu M. Designing high-performance storage in HfO2/BiFeO3 memristor for artificial synapse applications. Adv Electron Mater. 2020;6:1901012. https://doi.org/10.1002/aelm.201901012.
61. Lee S, Wolfe S, Torres J, Yun M, Lee J-K. Asymmetric bipolar resistive switching of halide perovskite film in contact with TiO2 layer. ACS Appl Mater Interfaces. 2021;13:27209–16. https://doi.org/10.1021/acsami.1c06278.
62. Muthu C, Resmi AN, Pious JK, Dayal G, Krishna N, Jinesh KB, Vijayakumar C. Resistive switching in formamidinium lead iodide perovskite nanocrystals: a contradiction to the bulk form. J Mater Chem C. 2021;9:288–93. https://doi.org/10.1039/D0TC03275A.
63. Huang Y, Tang L, Wang C, Fan H, Zhao Z, Wu H, Xu M, Shen R, Yang Y, Bian J. Triple-cation perovskite resistive switching memory with enhanced endurance and retention. ACS Appl Electron Mater. 2020;2:3695–703. https://doi.org/10.1021/acsaelm.0c00674.
64. Xiong Z, Hu W, She Y, Lin Q, Hu L, Tang X, Sun K. Air-stable lead-free perovskite thin film based on CsBi3I10 and its application in resistive switching devices. ACS Appl Mater Interfaces. 2019;11:30037–44. https://doi.org/10.1021/acsami.9b09080.
65. Pawara P, Okafor E, Groefsema M, He S, Schomaker LRB, Wiering MA. One-vs-One classification for deep neural networks. Pattern Recognit. 2020;108:107528. https://doi.org/10.1016/j.patcog.2020.107528.
66. Rifkin R, Klautau A. In defense of one-vs-all classification. J Mach Learn Res. 2004;5:101–41.
67. Prezioso M, Merrikh Bayat F, Hoskins B, Likharev K, Strukov D. Self-adaptive spike-time-dependent plasticity of metal-oxide memristors. Sci Rep. 2016;6:21331. https://doi.org/10.1038/srep21331.
68. Wang T-Y, Meng J-L, Li Q-X, He Z-Y, Zhu H, Ji L, Sun Q-Q, Chen L, Zhang DW. Reconfigurable optoelectronic memristor for in-sensor computing applications. Nano Energy. 2021;89:106291. https://doi.org/10.1016/j.nanoen.2021.106291.
69. Kanno K, Uchida A. Photonic reinforcement learning based on optoelectronic reservoir computing. Sci Rep. 2022;12:3720. https://doi.org/10.1038/s41598-022-07404-z.
70. Tan H, Liu G, Zhu X, Yang H, Chen B, Chen X, Shang J, Lu WD, Wu Y, Li R-W. An optoelectronic resistive switching memory with integrated demodulating and arithmetic functions. Adv Mater. 2015;27:2797–803. https://doi.org/10.1002/adma.201500039.
71. Tan H, Liu G, Yang H, Yi X, Pan L, Shang J, Long S, Liu M, Wu Y, Li R-W. Light-gated memristor with integrated logic and memory functions. ACS Nano. 2017;11:11298–305. https://doi.org/10.1021/acsnano.7b05762.
72. Tan H, Liu G, Li R-W, Tan H, Liu G, Li R-W. Multifunctional optoelectronic device based on resistive switching effects. In: Srivastava R, editor. Recent development in optoelectronic devices. London: IntechOpen; 2018. https://doi.org/10.5772/intechopen.74826.
73. Luo Z-D, Xia X, Yang M-M, Wilson NR, Gruverman A, Alexe M. Artificial optoelectronic synapses based on ferroelectric field-effect enabled 2D transition metal dichalcogenide memristive transistors. ACS Nano. 2020;14:746–54. https://doi.org/10.1021/acsnano.9b07687.
74. Marreiros AC, Daunizeau J, Kiebel SJ, Friston KJ. Population dynamics: variance and the sigmoid activation function. Neuroimage. 2008;42:147–57. https://doi.org/10.1016/j.neuroimage.2008.04.239.
75. Deng L. The MNIST database of handwritten digit images for machine learning research [Best of the Web]. IEEE Signal Process Mag. 2012;29:141–2. https://doi.org/10.1109/MSP.2012.2211477.
76. Pietrzak P, Szczęsny S, Huderek D, Przyborowski Ł. Overview of spiking neural network learning approaches and their computational complexities. Sensors. 2023;23:3037. https://doi.org/10.3390/s23063037.
77. Eshraghian JK, Ward M, Neftci EO, Wang X, Lenz G, Dwivedi G, Bennamoun M, Jeong DS, Lu WD. Training spiking neural networks using lessons from deep learning. Proc IEEE. 2023;111:1016–54. https://doi.org/10.1109/JPROC.2023.3308088.
78. Lu S, Xu F. Linear leaky-integrate-and-fire neuron model based spiking neural networks and its mapping relationship to deep neural networks. Front Neurosci. 2022. https://doi.org/10.3389/fnins.2022.857513.